RESULTS OF THE SHORT PULSE DRIVEN LLNL/UCLA IFEL EXPERIMENT*

J.T. Moody, P. Musumeci
Department of Physics and Astronomy, UCLA, Los Angeles California, USA
G.G. Anderson, S.G. Anderson, S. Betts, S. Fisher, D. Gibson, A. Tremaine, and S. Wu
Lawrence Livermore National Laboratory, Livermore, California, USA

Abstract

The results of the LLNL/UCLA inverse free electron laser (IFEL) experiment are presented. A 500 mJ 120 fs Ti:Saph laser pulse interacts with a short electron beam in a planar undulator tapered both in magnetic field strength and period to accelerate the electron beam. The tapering of the undulator maintains resonant energy exchange between the laser and electron beam while the electron beam's energy increases. We observe an energy modulation from 77 MeV to 120 MeV. Through use of simulations that are consistent with the observed data, we report a peak acceleration gradient of at least 180 MeV/m.

INTRODUCTION

The growing expense of high energy electron accelerators has produced a demand for increasingly compact, high gradient accelerators than traditional rf accelerators. Because of breakdown which occurs at around 100 MeV/m for traditional rf structures, shorter wavelengths must be used to drive the acceleration. The inverse free electron laser (IFEL) [1] is a laser driven electron accelerating scheme that has the advantage of taking place in vacuum.

In this acceleration scheme, a high intensity laser copropagates with a relativistic electron beam through an undulator. As the electron beam oscillates in the periodic magnetic field, it's transverse velocity allows for coupling to the laser's transverse electric field. If the laser's frequency, electron beams energy, and the magnetic field's strength and period are set such that the electron beam slips one laser wavelength per undulator period, energy is maximally transferred between the laser and the electron beam. As the electron beam becomes accelerated by this period averaged effect, the undulator must be tapered in order to maintain the resonance condition and facilitate efficient energy exchange.

This concept was demonstrated at Neptune at UCLA [2], as well as STELLA at Brookhaven National Lab (BNL) [3]. Renewed interest in IFEL has allowed experiments to be performed at Lawrence Livermore National Lab and BNL. While BNL's Rubicon [4] focused on use of a helical undulator to give stronger coupling to a circularly polarized CO_2 laser at low rep rate (.05Hz), the LLNL IFEL Project focuses on exploiting the high repetition rate of TW class Titanium Sapphire laser systems (10 Hz) and achieving high gradient acceleration with a sub picosecond driving laser. This paper covers the preliminary results of the LLNL IFEL experiment.

THEORETICAL BACKGROUND

If we define a pondermotive phase as $\Psi = (k + k_w)z - \omega t - \Phi_G$, we can use this phase as the coordinate of an electron in the period averaged pondermotive field. Here k and k_w are the radiation wave number and undulator wave number, respectively, and ω is the radiation frequency, and Φ_G is the Guoy phase shift.The electron's conjugate momentum then can be described by γ, the electron's energy normalized by it's rest energy. The longitudinal equations of motion then can be described by:

$$\frac{d\gamma}{dz} = \frac{1}{2\gamma} k K_L K J J sin\Psi \tag{1}$$

$$\frac{d\Psi}{dz} = k_w - k\frac{1+\frac{K^2}{2}}{2\gamma^2} - \frac{1}{z_r(1+\frac{z}{z_r}^2)} \tag{2}$$

Where K_L is the radiation parameter equal to eE_0/kmc^2 and E_0 is the peak radiation electric field, m is the electron mass, and c is the speed of light. K is the undulator strength parameter and is equal to $eB_w/k_w mc^2$ and B_w is the peak undulator magnetic field. JJ is the coupling factor, which is a result of using a planar undulator. z_r is the Rayleigh range, and the final term in the pondermotive phase evolution is due to the Guoy phase shift.

If we allow the left hand side of Eq. 2 to go to zero, this gives the condition for which the pondermotive phase does not evolve. γ_r is then resonant electron's normalized energy. Plugging into Eq. 1 we have a description of evolution of a resonant particle as it is accelerated with a stationary phase. Expanding about the resonant phase,Ψ_r, we have a pondermotive potential that goes like $cos\Psi + \Psi sin(\Psi_r)$. This potential creates a stable accelerating bucket whose width in phase is dependent on the resonant phase. If the resonant phase is near zero, the bucket is wide and traps many particles at the cost of reduced accelerating gradient whereas if the resonant phase is near $\pi/2$ then the gradient is maximum but only a single point in phase space can be accelerated. If the laser intensity is not matched to the design, the injected electrons can fall out of the pondermotive bucket and resonant acceleration ceases. Non trapped particles interaction increases the energy spread of the non-captured distribution. Beyond the 1-D equations of motion, the particle tracking code cbeam [5] was used together with

* This work supported by US DOE Grant DE-FG02-92ER40693,Defense of Threat Reduction Agency award HDTRA1-10-1-0073 and University of California Office of the President award 09-LR-04-117055-MUSP.

Parmela [6]and Elegant[7] to model the evolution of the electron beam in a start-to-end simulation. The results of the integration of the equations of motion in the pondermotive phase description matched the start-to-end simulation well.

EXPERIMENTAL DESCRIPTION

A layout of the interaction area can be seen in Fig 1. The electron beam approaches from the left of the diagram after being accelerated to injection energy and acquiring longitudinal chirp appropriate for compression. The electron beam is then compressed by the chicane and put on axis for the final focus quadrupole magnets that focus that electron beam at the center of the undulator to a spot size of 100 µm. The laser approaches from the right of the diagram and Spatial overlap between the electron beam and laser is achieved using DRZ fluorescent screens before and after the undulator, as well as a finger at the center of the undulator. Synchronicity to 2 ps between the electron beam and laser pulse is achieved by observing the optical transition radiation and laser in a streak camera. A micrometer on the delay arm on the interaction laser is then slowly scanned until electron beam modulation is observed. Experimental parameters can be seen in Table 1.

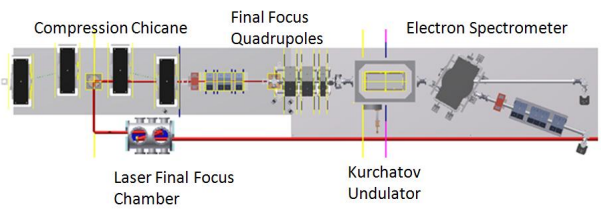

Figure 1: CAD Model of IFEL Interaction Region.

The LLNL BLDG 194 beamline consists of a SLAC/UCLA/BNL 1.6 Cell S-Band photogun, acceleration by three 3 m SLAC style accelerating sections, chirped for compression by a final accelerating section compressed through a chicane, and focused into the undulator. With the radius of 1 mm a 120 fs laser pulse applied to the cathode, the electron beam is produced in the photoinjector blowout regime, in which the electron beam expands nonlinearly into a near uniformly filled ellipsoid, helping to preserve transverse and longitudinal emittance during initial acceleration.

The KIAE-2p hybrid planar undulator was used in this experiment. Built by the Kurchatov Institute and originally designed for the UCLA Neptune IFEL experiment[2], the aggressively tapered undulator was designed for a 3.5 cm Rayleigh Range. It is nonlinearly tapered in both field strength and undulator period.

The Ti:Saph laser was purchased from Amplitude Technologies [8]. The laser consists of an SHG fiber oscillator, a regenerative amplifier 4 pass amplifier, and compressor. The spot size which is larger than the diffraction limited case, is a result of higher order modes acquired in the main amplifier, resulting in an M^2 value of approximately 1.3. The laser waist parameters shown in Table 1 were measured by attenuating it at low power and putting it directly into a CCD camera. The camera was moved along a linear stage and the Rayleigh range, minimum spot and a degree of astigmatism were measured.

Determination of energy modulation for the high gradient IFEL requires a broadband spectrometer. The spectrometer was made by placing a DRZ fluorescent pop-in within the tank of the dipole magnet. Such a broadband spectrometer has a nonlinear calibration, which was determined by sweeping the magnetic field for a fixed momentum electron beam and determining the various bend radii. A simple geometrical model was developed to ensure accuracy of the spectrometer. The method of calibration data was well matched with the model.

Table 1: IFEL Experimental Parameters

Beam Parameters	
Average Injection Energy	55-77 MeV
Charge	50 pC
Undulator Parameters	
K_0	0.2
K_f	2.8
λ_{w0}	1.5 cm
λ_{wf}	5.0 cm
L_w	50 cm
Laser Parameters	
λ	785 nm
τ	150 fs
Pulse Energy	500 mJ
z_r	12 cm
w_0	200 µm

EXPERIMENTAL RESULTS

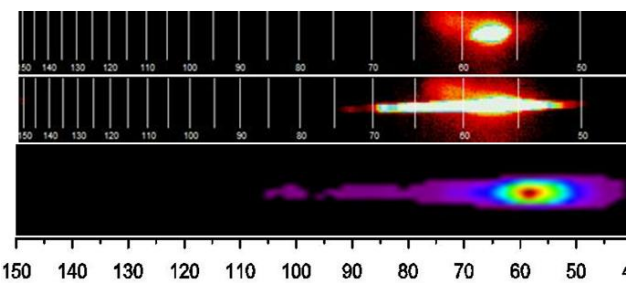

Figure 2: 57 MeV IFEL Interaction Results. a. Electron beam without laser. b. Electron beam with laser applied, IFEL interaction. c. 2D histogram binning of comparable simulation results. Horizontal Scale is Energy in MeV, measured data has nonlinear scaling.

We placed the waist of the laser approximately 2 cm upstream of the center of the undulator and used 57 MeV injection energy into the IFEL. Placing the waist further up-

ISBN 978-3-95450-138-0

stream allows for capture earlier in the undulator at the cost of dropping off of the resonant energy curve faster. The energy modulation can be seen in Fig. 2. For both sets the images data has a nonlinear scale by nature of the spectrometer while the simulation data has a linear scale.

We then placed the waist at the center of the undulator and injected at 77 MeV, the highest energy our chicane compressor will allow, injecting into the undulator at above initial resonant energy. The results from this interaction can be seen on Fig. 3. In both cases simulations were run with the measured laser waist parameters. The simulation spectra matched the observed spectra fairly well, justifying the examination of the simulation data as acceleration occurs in the undulator.

Figure 4 shows the average energy evolution for the particles gaining the most energy in three simulations: the design case with a 3.5 cm Rayleigh range 100 µm laser waist is used, and the two cases for our measured waist parameters at the two observed energies. The lower bound energy cuts were 180, 110 and 70 MeV for the design, 77 and 57 MeV cases, respectively. The peak gradient of the 77 MeV injected energy curve shows a maximum gradient of 180 MeV/m. While the design curve shows resonant gain throughout the undulator, the 77 and 57 MeV cases show the electron beam accelerated up to a point where there is a sharp change in slope as the electrons fall out of the pondermotive bucket in the first half of the undulator. After the electrons fall out of the pondermotive bucket nonresonant energy modulation occurs to further increase the energy spread, showing mild gain based upon the selection of the highest energy particles.

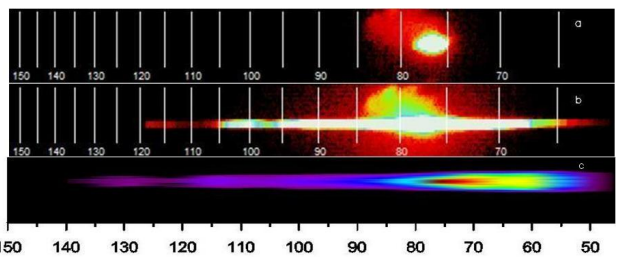

Figure 3: 77 MeV IFEL Interaction Results.a. Electron beam without laser. b. Electron beam with laser applied, IFEL interaction. c. 2D histogram binning of comparable simulation results. Horizontal Scale is Energy in MeV, measured data has nonlinear scaling.

CONCLUSION AND FURTHER STUDY

The IFEL interaction has been demonstrated and has produced high peak gradient acceleration (180 MeV/m) and a record maximum energy produced by the IFEL acceleration mechanism of 120 MeV. Further improvement of the laser waist should yield a higher gradient over the entire undulator with acceleration to the design energy. The short pulse nature of the Ti:Sapphire IFEL is planned to be investigated over the next few months with an electrooptic

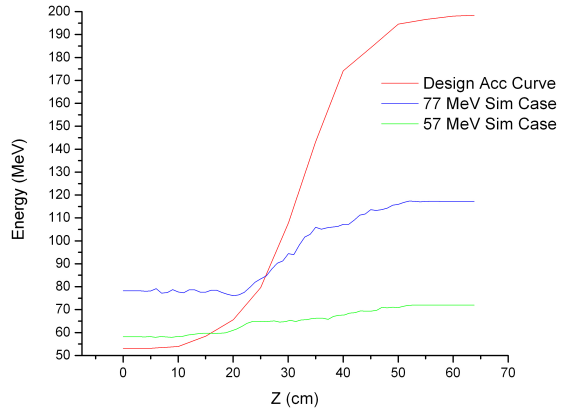

Figure 4: Acceleration curves for the design laser and injection at 50 MeV, The 57 MeV case, and the 77 MeV case.

sampling based time of arrival diagnostic discussed in previous work.[9]. The electrooptic sampling diagnostic will allow for relative time of arrival measurements to be correlated with the observed energy modulation so that the time of arrival jitter can be unfolded from the temporal overlap tolerance.

REFERENCES

[1] E.D. Courant, C. Pellegrini, and W. Zakowicz. High-energy inverse free electron laser accelerator. Physical Review A, 32:2813, 1985.

[2] P. Musumeci et al., High Energy Gain of Trapped Electrons in a Tapered, Diffraction-Dominated Inverse-Free-Electron Laser, Physical Review Letters, 94:154801, (20 April 2005).

[3] Kimura, W. D. et al., 2004b First demonstration of hightrapping efficiency and narrow energy spread in a laser-driven accelerator. Phys. Rev. Lett. 92, 054 801.

[4] J. Duris et al., High Energy Gain of Electrons in a High Gradient Helical Inverse Free Electron Laser PRL (submitted August 2013).

[5] S. Anderson et al., Proc of PAC2011 (2011).

[6] L.Young and J. Billen, The Particle Tracking Code PARMELA, PAC03 Proceedings, May 2003

[7] M. Borland, elegant: A Flexible SDDS-Compliant Code for Accelerator Simulation, Advanced Photon Source LS-287, September 2000.

[8] Amplitude Technologies: `www.amplitude-technologies.com/`

[9] J. Moody et al., Proc of IPAC 2012 (2012)